Journal of Dental Research
2018, Vol. 97(3) 329–337

DOI: 10.1177/0022034517735094
journals.sagepub.com/home/jdr

Fibrocartilage Stem Cells Engraft and Self-Organize into Vascularized Bone

J. Nathan[1], A. Ruscitto[1], S. Pylawka[1], A. Sohraby[1], C.J. Shawber[2], and M.C. Embree[1]

Abstract

Angiogenesis is a complex, multicellular process that is critical for bone development and generation. Endochondral ossification depends on an avascular cartilage template that completely remodels into vascularized bone and involves a dynamic interplay among chondrocytes, osteoblasts, and endothelial cells. We have discovered fibrocartilage stem cells (FCSCs) derived from the temporomandibular joint (TMJ) mandibular condyle that generates cartilage anlagen, which is subsequently remodeled into vascularized bone using an ectopic transplantation model. Here we explore FCSC and endothelial cell interactions during vascularized bone formation. We found that a single FCSC colony formed transient cartilage and host endothelial cells may participate in bone angiogenesis upon subcutaneous transplantation in a nude mouse. FCSCs produced an abundance of the proangiogenic growth factor vascular endothelial growth factor A and promoted the proliferation of human umbilical vein endothelial cells (HUVECs). Using a fibrinogen gel bead angiogenesis assay experiment, FCSC cell feeder layer induced HUVECs to form significantly shorter and less sprouts than D551 fibroblast controls, suggesting that FCSCs may initially inhibit angiogenesis to allow for avascular cartilage formation. Conversely, direct FCSC-HUVEC contact significantly enhanced the osteogenic differentiation of FCSCs. To corroborate this idea, upon transplantation of FCSCs into a bone defect microenvironment, FCSCs engrafted and regenerated intramembranous bone. Taken together, we demonstrate that the interactions between FCSCs and endothelial cells are essential for FCSC-derived vascularized bone formation. A comprehensive understanding of the environmental cues that regulate FCSC fate decisions may contribute to deciphering the mechanisms underlying the role of FCSCs in regulating bone formation.

Keywords: bone remodeling/regeneration, angiogenesis, regeneration, TMJ, cartilage, endothelial cells

Introduction

There are 2 distinct classical bone developmental processes (Erlebacher et al. 1995). Endochondral ossification forms the axial skeleton, cranial base, and posterior skull, while intramembranous ossification forms the flat bones of the skull and part of the clavicle (Berendsen and Olsen 2015). During intramembranous ossification, a condensation of mesenchymal stem cells accumulates and directly differentiates into osteoblasts that form new bone (Erlebacher et al. 1995). Comparatively, endochondral ossification relies on an avascular cartilage template that is subsequently remodeled into bone (Kronenberg 2003). During the former, the transition from cartilage to bone is an intricate, multicellular process that is by and large marked by blood vessel invasion of the avascular cartilage template (Schenk et al. 1968; Carlevaro et al. 2000). Cartilage tissue plays a vital role in the regulation of angiogenesis, where proliferating chondrocytes inhibit angiogenesis (Bi et al. 1999; Shukunami and Hiraki 2007; Hattori et al. 2010), while hypertrophic chondrocytes secrete proangiogenic cues to recruit blood vessel invasion and osteoblasts (Schipani et al. 2009; Lee et al. 2012).

Both bone developmental processes form the mandible. The mandibular body is formed by intramembranous ossification, while the posterior components, including the angle, coronoid process, and condyle, are formed using a cartilage template (Tomo et al. 1997; Ramaesh and Bard 2003). Mandibular condylar cartilage is marked by growth defined by cellular zones of maturation, including the fibrocartilaginous superficial zone, polymorphic zone, maturation zone, and hypertrophic zone (Shibukawa et al. 2007).

Our lab has discovered that fibrocartilage stem cells (FCSCs) reside in the superficial zone niche of the temporomandibular joint (TMJ) mandibular condyle (Embree et al. 2016). Using an in vivo xenograft model, we found that transplanted FCSCs form transient cartilage anlagen that completely remodels into trabecular bone-like tissue (Embree et al.

[1]TMJ Biology and Regenerative Medicine Laboratory, College of Dental Medicine, Columbia University Medical Center, New York, NY, USA
[2]Department of OB/GYN, Division of Reproductive Sciences, College of Physicians and Surgeons, Columbia University Medical Center, New York, NY, USA

A supplemental appendix to this article is available online.

Corresponding Author:
M.C. Embree, TMJ Biology and Regenerative Medicine Laboratory, College of Dental Medicine, Columbia University Medical Center, 630 W. 168 St., P&S 16-440, New York, NY 10032, USA.
Email: mce2123@cumc.columbia.edu

2016). Thus, we speculate that FCSCs recapitulate a bone developmental process similar to endochondral ossification. Given blood supply is a critical feature that differentiates cartilage from bone (Vu et al. 1998; Gerber et al. 1999), here we explore the relationship between FCSCs and endothelial cells in vascularized bone formation. A deeper understanding of the biological and environmental cues that regulate FCSC fate decisions toward bone may contribute to deciphering the mechanisms underlying FCSCs' behavior in disease and in skeletal repair.

Materials and Methods

Animals

All animal procedures were performed using female athymic nude mice 6 to 8 wk old (n = 30) and male Sprague Dawley male rats ages 6 to 8 wk old (n = 8 rats) with approval from the Institutional Animal Care and Use Committee (IACUC) at Columbia University (AC-AAAF503 and AC-AAAF4205). The 8-wk-old transgenic rat GFP (Marano et al. 2008) tissues (n = 6 rats) were kindly provided by Dr. Dongming Sun (Rutgers University, New Brunswick New Jersey, USA).

Cell Isolation and Culture

FCSCs and bone marrow stromal cells were isolated from Sprague Dawley rats (Embree et al. 2016). Single-cell suspensions were cultured (5% CO_2, 37°C) in Dulbecco's modified Eagle's medium (DMEM) (11885-092; Invitrogen) supplemented with 20% lot-selected fetal bovine serum (FBS) (HyClone), glutamax (35050-061; Invitrogen), penicillin-streptomycin (15140-163; Invitrogen), and 2-mercaptoethanol (Gibco) for 4 to 6 d. Primary human umbilical vein endothelial cells (HUVECs) were kindly provided by Dr. Jan Kitajewski (Columbia University) and maintained on collagen I (Corning)–coated plates in EGM-2 media (CC-4176; Lonza). Human D551 fibroblasts (ATCC) were maintained in DMEM (Gibco), 10% heat-inactivated FBS, and penicillin-streptomycin. FCSCs, bone marrow stromal cells (BMSCs), and D551 fibroblasts were cultured in EGM-2 until 100% confluent, and conditioned media (CM) were collected for use in the HUVEC growth curve and scratch migration assay. For growth curve, HUVECs were cultured in FCSC-CM, D551-CM, and BMSC-CM. HUVECs were counted daily for 4 d. HUVEC migration was measured by an in vitro scratch assay (Liang et al. 2007) using HUVECs cultured in FCSC-CM, D551-CM, and BMSC-CM. Scratches were imaged every 4 h for 12 h, and the scratch area was measured using Olympus cellSens Dimension imaging software.

Histology and Immunohistochemistry

Samples were fixed in 4% paraformaldehyde, decalcified in ethylenediaminetetraacetic acid (EDTA), and prepared for paraffin or frozen sections. For immunohistochemistry, sections were treated with Chondroitinase ABC (C3667-10UN; Fisher) and immunolabeled with antibodies: CD31 (ab28364, 1:100; Abcam) and osteocalcin (AB10911, 1:100; Millipore) at 4°C overnight followed by secondary antibody (A-11010, 1:1000; Invitrogen). Isotype-matched antibodies were used as negative controls.

Fluorescence-Activated Cell Sorting Analysis

All cell sorting was performed at the Columbia Center for Translational Immunology Flow Cytometry Core (CCTI, Columbia University Medical Center, New York, NY, USA). BD Influx cell sorter was used to isolate single GFP^+ FCSCs into 96-well plates.

RNA Isolation and Quantitative Reverse Transcription Polymerase Chain Reaction

Total RNA was purified (12183018A; Ambion) and treated with DNAse I (AM2222; Ambion). RNA samples (260/280 ≥1.8) were used to obtain complementary DNA (cDNA) (AM2222; Bio-Rad). Quantitative reverse transcription polymerase chain reaction (qRT-PCR) was performed using TaqMan Universal PCR Master Mix (4304437; Applied Biosystems) and predesigned rat primers (Applied Biosystems) for *Bsp* (Rn00561414_m1), *Ocn* (Rn01455285_g1), *Runx2* (Rn01512298_m1), *Acan* (Rn00573424_m1), *Fgf1* (Rn00689153_m1), and *Vegfa* (Rn01511602_m1). Gene expression levels were normalized to housekeeping gene *Gapdh* (Rn01775763_g1*; Applied Biosystems).

Fibrinogen Gel Bead Angiogenesis Assay

Fibrinogen gel bead angiogenesis assay (FIBA) was performed as described (Nakatsu and Hughes 2008; Tattersall et al. 2016). HUVECs were transduced with a lentivirus encoding red fluorescence protein (RFP) (Tattersall et al. 2016). Briefly, HUVEC-coated beads (400 cells/bead) were washed in EGM-2 ± FCSCs and resuspended in fibrinogen solution (Sigma-Aldrich) (150 beads/500 µL fibrinogen solution). D551 fibroblasts or FCSCs served as feeder cells (1×10^5/well). Olympus cellSens Dimension software was used to quantify the number of sprouts/bead, sprout length from the bead base to tip, and caliber at sprout the midpoint.

Vascular Endothelial Growth Factor A Enzyme-Linked Immunosorbent Assay

FCSCs (5×10^4/well) were seeded onto 24-well plates in basal media with 10% FBS or EGM-2 (CC-4176; Lonza). Vascular endothelial growth factor A (VEGF-A) was measured in FCSC cell culture supernatants using enzyme-linked immunosorbent assay (ELISA) (ab100786; Abcam).

Osteogenesis Co-culture Assay

FCSCs and HUVECs were co-cultured in direct contact at various FCSC/HUVEC ratios (1:1, 2:1, 1:2) and compared to

FCSCs alone. The FCSC/HUVEC groups were seeded using the same initial total cell number (2×10^5/well in 24-well plate) using EGM-2 media and cultured until confluent. Medium was replaced with osteogenic induction media (Bi et al. 2007; Embree et al. 2016). Osteogenesis was evaluated after 1 wk via 2% Alizarin red S (pH 4.2; Sigma-Aldrich), alkaline phosphatase assay (ab83369; Abcam), and qRT-PCR using total RNA derived from FCSCs and HUVECs.

Transwell Noncontact Osteogenesis Assay

Transwell Permeable Supports (Transwell 3470; Corning) were used for the paracrine, noncontact FCSC/HUVEC co-culture assay. HUVECs were seeded onto Transwell Permeable inserts and FCSCs were seeded into the well beneath the insert in a 24-well plate using a 2:1 or 1:1 ratio of FCSC/HUVECs with the same total cell density (3.75×10^5/well) and compared to FCSCs cultured alone (1:0). Cells were cultured at a density that ensured FCSC confluency in 1 d followed by culture in osteogenic media for 8 d. qRT-PCR using total RNA derived from rat FCSCs was used to assess FCSC osteogenic differentiation.

Ectopic Transplantation

FCSCs or single-cell colonies (2.0×10^6) were seeded onto a collagen sponge (12 × 12 × 3 mm; 1690ZZ; Helistat) and transplanted onto the dorsum of female, athymic nude mice (Harlen Athymic Nude-Foxn1^{nu}). Transplants were harvested after 4 wk ($n = 6$) and 8 wk ($n = 8$ mice) for analysis.

Calvarial Defect Model

To create the calvarial defect, periosteum was removed, and a 4-mm defect was made in the parietal bone of female athymic nude mice (Harlen Athymic Nude-Foxn1^{nu}) using a trephine bur while maintaining dura mater and excluding suture. Collagen sponges (4 × 4 × 1.5 mm) seeded with GFP$^+$ FCSCs (2.0×10^6) or no cells were transplanted into the defect. Transplants were analyzed after 4 wk ($n = 8$ female mice) and 8 wk ($n = 8$ female mice).

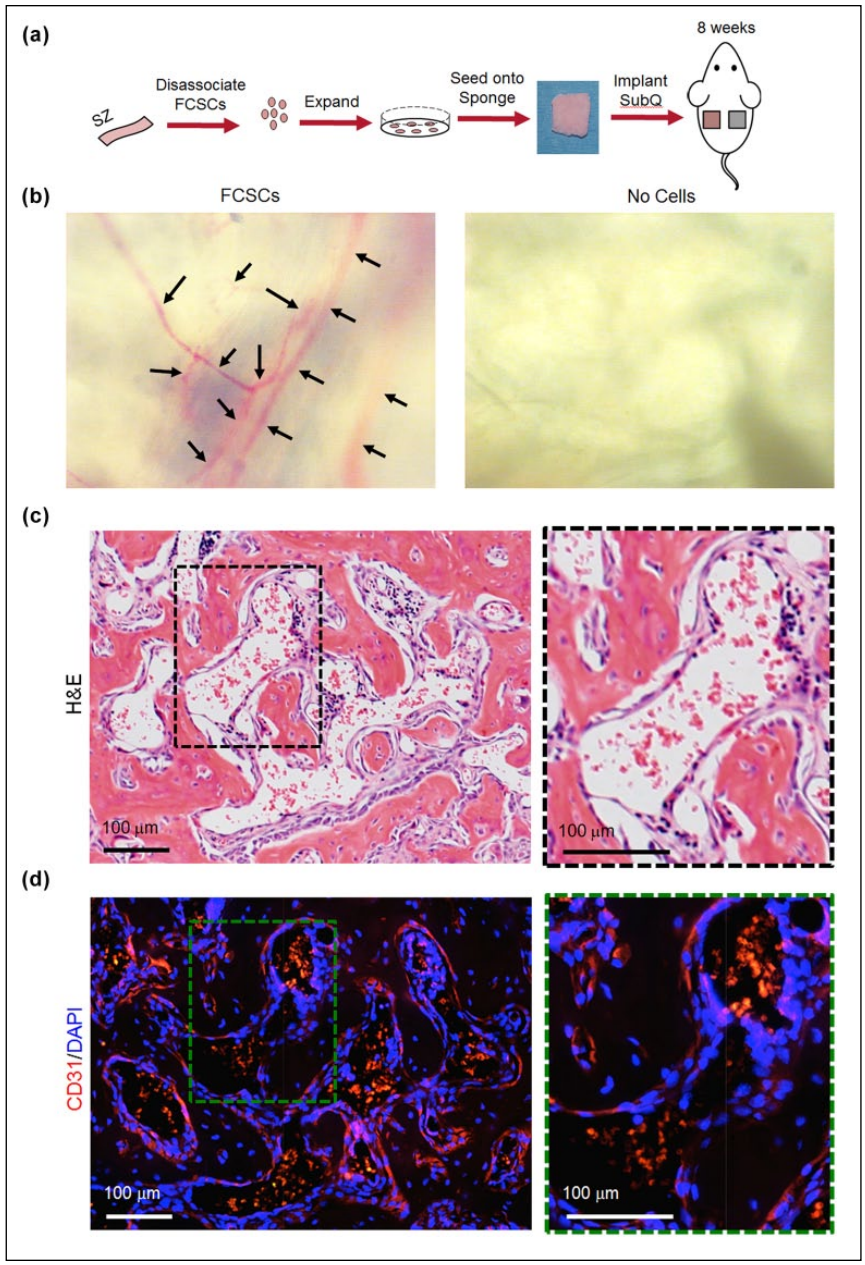

Figure 1. Heterogeneous fibrocartilage stem cells (FCSCs) self-organize into vascularized bone-like tissue in a xenograft model at 8 wk. (**a**) Schematic demonstrating FCSC transplantation experiment. FCSCs were isolated from rat temporomandibular joint (TMJ) superficial zone (SZ) tissue, digested, expanded, seeded onto a collagen sponge, and transplanted on dorsum of nude mice for 8 wk. Transplanted collagen sponge with no cells served as a negative control. (**b**) Superior view of collagen sponges after 8 wk showed that FCSC transplants recruited blood vessels. (**c**) Representative hematoxylin and eosin (H&E) staining of FCSC transplants after 8 wk showed FCSCs spontaneously generated vascularized bone-like tissue. Black dashed box is shown in higher magnification on the right. Scale bar = 100 µm. (**d**) Immunohistochemistry for CD31 showed the presence of endothelial cells and new blood vessel–like formation. Green dashed box is shown in higher magnification on the right. Scale bar = 100 µm.

Statistical Analysis

All statistics were calculated using Prism 6 (GraphPad Software). The statistical significance between 2 groups was determined using the paired Student's *t* test assuming Gaussian

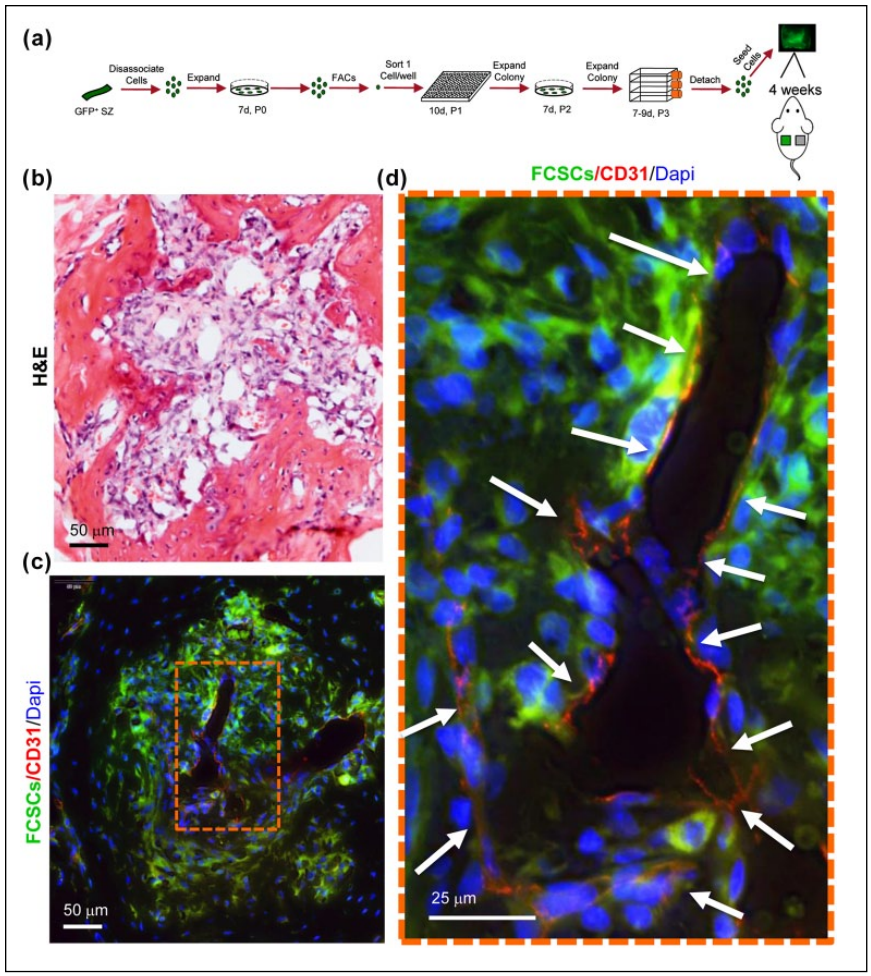

Figure 2. A single fibrocartilage stem cell (FCSC) supports host blood vessel formation during transition from cartilage to bone in xenograft model at 4 wk. (**a**) Schematic showing single FCSC isolation. Heterogeneous GFP$^+$ FCSCs were derived from the temporomandibular joint (TMJ) superficial zone (SZ) tissue from a GFP transgenic rat. GFP$^+$ FCSCs were expanded in vitro and fluorescence-activated cell sorting (FACS) was used to plate a single cell/well into a 96-well plate. A total of 17 single-cell colonies were expanded over passages 2 to 3, seeded onto a collagen sponge, and surgically transplanted subcutaneously on the dorsum of nude mice for 4 wk. (**b**) Representative hematoxylin and eosin (H&E) stain of 2 of 17 xenografts at 4 wk showing transition to vascularized bone-like tissue at 4 wk. Scale bar = 50 µm. (**c**) Immunohistochemistry of CD31 (red) shows new blood vessel formation (arrows) surrounded by GFP$^+$ FCSCs. (**d**) Orange dashed box is shown in higher magnification on the right. Scale bar = 50 µm and 25 µm, respectively.

distribution. The normality of distribution was confirmed using the Kolmogorov-Smirnov test, and the resulting 2-tailed P value ≤0.05 was regarded as a statistically significant difference. Among 3 groups, 1-way analysis of variance (ANOVA) followed by Tukey's post hoc test was used. For multiple comparisons, a 2-way ANOVA followed by Tukey's post hoc or Bonferroni's post hoc test was used.

Results

FCSCs Self-Organize into Vascularized Bone-Like Tissue

We have previously shown that FCSCs isolated from the superficial zone of the TMJ condyle self-organize into cartilage and transition to bone after 4 wk; by 8 wk, FCSCs form trabecular bone with marrow-like spaces using an in vivo transplantation model (Embree et al. 2016). We thus examined the vascular phenotype in FCSC xenografts at the 8-wk time point, representing peak bone formation (Embree et al. 2016) (Fig. 1a). Collagen sponges with no cells were transplanted in the contralateral flank as a control. After 8 wk, blood vessels were observed on the surface in 7 of 8 collagen sponges with FCSCs, which was not observed in controls (Fig. 1b). FCSCs generated bone and organized a bone marrow–like niche (7/8 sponges; Fig. 1c) lined with CD31$^+$ endothelial cells (Fig. 1d, red). These data suggest that FCSCs may either form de novo blood vessels or recruit host cells to undergo angiogenesis.

A critical factor regulating cartilage remodeling into bone is new blood vessel formation (Descalzi Cancedda et al. 1995; Vu et al. 1998; Gerber et al. 1999; Hattori et al. 2010). We hypothesized that FCSCs recruit host endothelial cells to support FCSC transition from cartilage to bone at the 4-wk time point. To distinguish donor FCSCs from host cells, FCSCs were isolated from GFP rats (Marano et al. 2008). Fluorescence-activated cell sorting (FACS) was used to isolate 17 single-cell colonies of GFP$^+$ FCSCs that were expanded, seeded onto a collagen sponge, and transplanted subcutaneously on the dorsum of nude mice (Fig. 2a). The FCSC xenograft vascular phenotype was analyzed at 4 wk, a time point representing the peak transition of cartilage to bone (Embree et al. 2016). A total of 15 clones did not form cartilage or bone upon transplantation, thereby demonstrating the cell population heterogeneity. GFP$^+$ FCSCs surrounded CD31$^+$ endothelial cells, forming a blood vessel–like lumen (Fig. 2b–d). These data suggest that FCSCs recruit host endothelial cells to the transplant site, and angiogenesis may be a critical process that drives the transition of FCSC-derived cartilage into bone.

FCSCs Induce Proliferation of HUVECs

The in vivo xenograft model suggested that upon transitioning from cartilage to bone at the 4-wk time point, FCSC-derived chondrocytes and/or FCSC-derived osteoblasts might provide cues to support angiogenesis. Given the proangiogenic factor VEGF-A is highly expressed in hypertrophic chondrocytes and is critical for vascular bone formation (Zelzer et al. 2004; Duan

et al. 2015), we performed ELISAs to measure VEGF-A in the conditioned media collected from FCSCs. At 100% confluency, VEGF-A levels were 4-fold and 40-fold higher in FCSC-conditioned media relative to 10% FBS and EGM, respectively (Appendix Fig. 1), suggesting that FCSCs in culture may be proangiogenic.

Angiogenesis is a complex process that can be modeled in vitro using a FIBA (Nakatsu and Hughes 2008). In the FIBA experiment, HUVECs are bound to collagen-coated dextran beads and embedded in a fibrin clot, and the D551 fibroblast feeder layer provides angiogenic cues to induce HUVECs to form capillary lumen–containing structures (Nakatsu and Hughes 2008). Given FCSCs express VEGF-A (Appendix Fig. 1), we evaluated whether FCSCs could substitute D551 fibroblasts and promote angiogenesis in the FIBA. To distinguish HUVECs from FCSCs, a lentivirus encoding red fluorescence protein (RFP) was used to label HUVECs (Tattersall et al. 2016). After 4 d, HUVEC sprouting was not observed in the absence of a feeder layer (Fig. 3a). Relative to D551 fibroblasts, the FCSC feeder layer induced HUVECs to form a significantly lower number of sprouts with decreased length and uniform caliber (Fig. 3a–d). Although FCSCs express VEGF-A, they promoted angiogenic sprouting that was significantly less robust than that observed with D551 fibroblasts.

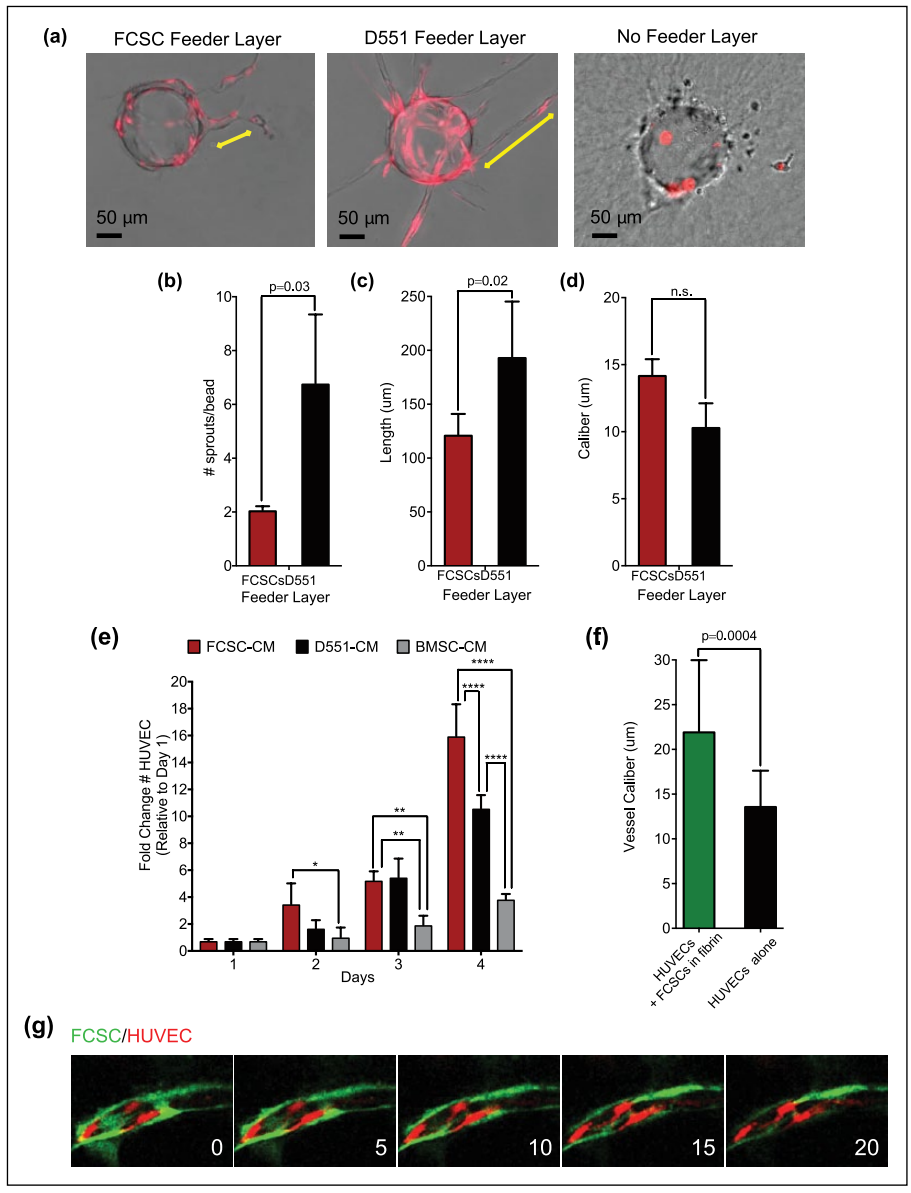

Figure 3. Fibrocartilage stem cells (FCSCs) induce proliferation of human umbilical vein endothelial cells (HUVECs), and direct FCSC-HUVEC association increases vessel caliber. FCSCs' ability to support angiogenesis was evaluated in vitro using a fibrin-induced bead angiogenesis assay (FIBA). HUVECs were transduced with a lentivirus encoding red fluorescence protein (RFP). HUVEC-coated beads were embedded in fibrin gel using either D551 fibroblasts or FCSCs as a cell feeder layer. (**a**) Representative images of beads with HUVEC sprouts from FIBA. Scale bar = 50 µm. CellSense Imaging Software was used to quantify the (**b**) number of sprouts per bead, (**c**) vessel length, and (**d**) vessel caliber. Data represented are mean ± SD; $n = 4$ experiments; paired Student's t test. (**e**) Growth curve of HUVECs cultured in conditioned media (CM) derived from fibrocartilage stem cells (FCSC-CM), D551 fibroblasts (D551-CMs), or bone marrow stromal cells (BMSC-CM). Data are mean ± SD; $n = 6$ experiments; $^{*}P \leq 0.03$, $^{**}P \leq 0.002$, $^{***}P \leq 0.0002$, $^{****}P \leq 0.0001$; 2-way analysis of variance followed by Tukey's post hoc test. (**f, g**) The effect of direct HUVEC-FCSC contact was investigated in a FIBA experiment where HUVEC-coated beads were embedded ± FCSCs within the fibrin clot. CellSense Imaging Software was used to quantify the (f) vessel caliber. (g) Sequential confocal microscopic images of FIBA experiment with direct HUVEC-FCSC contact showing GFP^{+} FCSC (green) localized to the luminal side of blood vessels derived from HUVECs (red).

The FIBA requires both HUVEC proliferation and migration that is promoted by VEGF-A; thus, we determined the effects of FCSC-CM on HUVEC growth and migration. FCSC-CM was compared to conditioned media from D551 fibroblasts (D551-CM) as a control and also to conditioned media from BMSC-CM, well-established bone-forming cells (Bianco and Robey 2015). To evaluate cell growth, HUVECs were seeded at subconfluency and maintained in different condition medias for 4 d. FCSC- CM induced a significant increase in the number of HUVECs relative to D551- CM and BMSC-CM (Fig. 3g). Using a scratch assay, there was no difference in HUVEC migration between FCSC-CM compared to D551-CM (Appendix Fig. 2). While FCSCs produce robust VEGF-A, other FCSC-derived factors may be contributing to HUVEC behavior (Sivaraj and Adams 2016). Taken together, these data suggest that indirect FCSC and HUVEC interactions have no

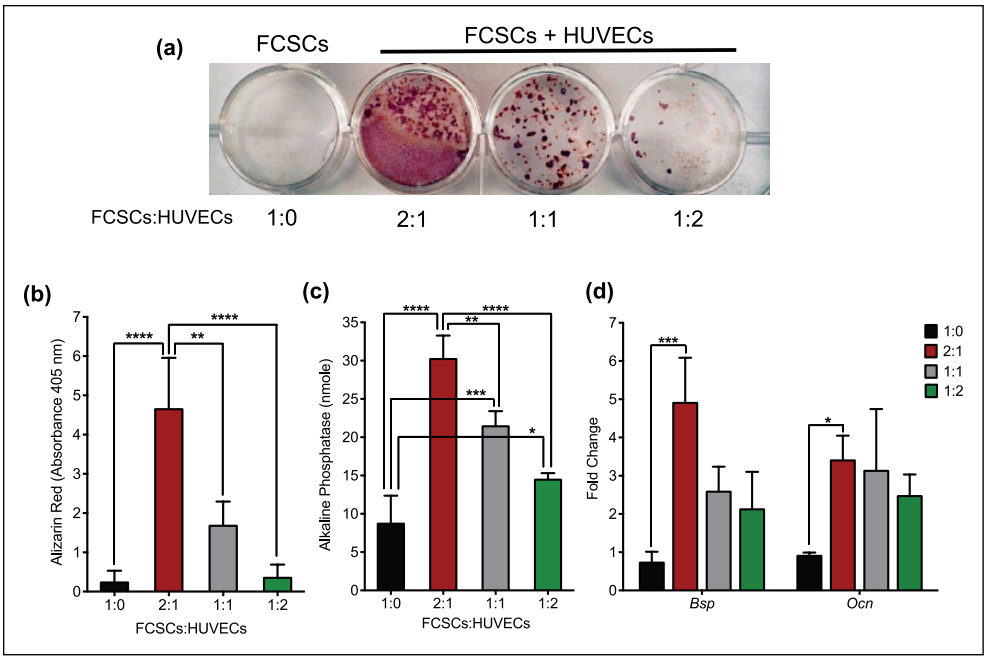

Figure 4. Human umbilical vein endothelial cells (HUVECs) enhance osteogenic differentiation of fibrocartilage stem cells (FCSCs). (**a**) Alizarin red staining of a calcium deposition assay with varying ratios of FCSCs and HUVECs co-cultured in osteogenic media for 2 wk. (**b**) Alizarin red staining was quantitated at an absorbance of 405 nm. Data are mean ± SD; $n = 4$ experiments; $^{*}P \le 0.05$, $^{**}P \le 0.01$, $^{***}P \le 0.001$, $^{****}P \le 0.0001$; 2-way analysis of variance (ANOVA) followed by Tukey's post hoc test. (**c**) Alkaline phosphatase assay with various concentrations of FCSCs and HUVECs co-cultured in osteogenic media for 1 wk. Data are mean ± SD; $n = 3$ experiments; $^{*}P \le 0.05$, $^{**}P \le 0.01$, $^{***}P \le 0.001$, $^{****}P \le 0.0001$; 2-way ANOVA followed by Tukey's post hoc test. (**d**) Quantitative reverse transcription polymerase chain reaction of FCSCs and HUVECs co-cultured in various proportions in osteogenic media for 1 wk. Data are normalized to glyceraldehyde 3-phosphate dehydrogenase (GAPDH) and mean fold change relative to FCSCs alone ± SD; $n = 3$ experiments; $^{*}P \le 0.05$; $^{***}P \le 0.001$; 2-way ANOVA followed by Tukey's post hoc test.

impact on HUVEC migration and impede angiogenesis. Thus, FCSCs' role in inhibiting angiogenesis may be a critical feature that allows FCSCs to initially form avascular cartilage as opposed to vascularized bone.

Direct FCSC-HUVEC Association Increases Vessel Caliber

In the FCSC xenograft model, GFP^{+} FCSCs were observed adjacent to CD31+ vessels (Fig. 2d). To mimic the in vivo conditions, we embedded FCSCs in the fibrin clot to evaluate their effect on angiogenesis in the FIBA experiment (Fig. 3f, g). After 4 d, addition of FCSCs to the fibrin clot correlated with a significant increase in the vessel caliber (Fig. 3f). Furthermore, GFP^{+} FCSCs were found to be closely associated with RFP-HUVECs in lumenized vessels (Fig. 3g). These data suggest that upon direct contact with HUVECs, FCSCs may function similar to perivascular cells to promote vessel lumenization and maturation (Tattersall et al. 2016). Thus, when FCSCs differentiate into bone and directly contact HUVECs, FCSCs may function to stabilize the blood vessels critical for bone maintenance and survival.

HUVECs Enhance Osteogenic Differentiation of FCSCs

Given endothelial cells promote osteogenesis of BMSCs (Villars et al. 2000), we determined the effects of HUVECs on FCSC osteogenesis. FCSCs and HUVECs were mixed together at varying ratios in suspension and cultured together using the same cell number in osteogenic media for 1 wk (Fig. 4). A 2:1 ratio of FCSC/HUVEC had a significantly higher calcium deposition than FCSCs alone in the Alizarin red assay (Fig. 4a, b). Consistent with this finding, the 2:1 ratio of FCSCs/HUVECs showed an increase in alkaline phosphatase activity, as well as expression of rat *Bsp* and *Ocn* transcripts using total RNA from mixed cultures (Fig. 4c, d). Conversely, HUVECs significantly inhibited the expression of the cartilage transcription factor *Sox9* in FCSCs at a 1:2 and 2:1 FCSCs/HUVECs ratio (Appendix Fig. 3). Together, these data suggest that FCSCs in direct contact with HUVECs have a higher osteogenic potential in comparison to FCSCs alone.

To examine whether HUVECs could induce FCSC osteogenesis through the secretion of noncontact-dependent paracrine factors, we cultured HUVECs on permeable Transwell membrane inserts and seeded FCSCs beneath inserts in osteogenic media for 8 d (Appendix Fig. 4). The expression of bone-related genes *Runx2, Bsp*, and *Ocn* was not significantly changed in FCSCs cultured with HUVEC-coated Transwells relative to FCSCs alone (Appendix Fig. 4). These data suggest that secreted factors produced by HUVECs were not sufficient to promote FCSC osteogenesis; thereby, HUVECs require direct contact with FCSCs to promote their osteogenic differentiation. Thus, in the absence of direct HUVEC contact, FCSCs may likely generate avascular cartilage as opposed to vascularized bone.

Transplanted FCSCs Engraft and Repair a Calvarial Bone Defect

Given the micro-environment niche is critical for determining stem cell fate specification (Bi et al. 2007) and direct FCSC

and HUVEC interactions promote osteogenic differentiation of FCSCs, we investigated whether a vascularized bone niche would direct FCSC toward an osteogenic lineage. GFP$^+$ FCSCs were transplanted into a mouse calvarial critical size defect model (Aalami et al. 2004) (Fig. 5a). Unlike our xenograft model (Embree et al. 2016), after 4 wk, no cartilage phenotype was observed (not shown). After 8 wk, gross macroscopic and radiographic analyses revealed bone-like tissue formed within the defect transplanted with FCSCs that was GFP$^+$ and radiopaque (Fig. 5b). Calvarial defects transplanted with cell-free sponges showed no bone-like tissue formed (Fig. 5c). GFP$^+$ FCSCs differentiated and formed de novo bone (DB) that expressed osteocalcin (OCN) (green box, Fig. 5d–f). At the periphery of the defect GFP$^+$ FCSCs, engraftment into the host bone (HB) was observed within the lacunae of DB (orange box, Fig. 5d, e, g). Immunohistochemistry showed that CD31$^+$ cells localized at the periphery of the FCSC engraftment area (white arrows, Fig. 5h), suggesting that FCSCs' integration is coupled with endothelial cell recruitment. These data show that FCSCs transplanted into a vascularized bone niche promotes FCSCs to self-organize into vascularized bone-like tissue.

Discussion

We demonstrate that heterogeneous FCSCs and 2 of 17 single FCSC clones formed vascularized bone-like tissue using an in vivo xenograft transplantation model. FCSCs are a heterogeneous population, and it is likely only a fraction of cells represents true stem/progenitor cells. To isolate FCSCs, we digested superficial zone tissue and expanded colony-forming cells using no specific identifying markers. We have previously shown that FCSCs expressed cell surface markers (Embree et al. 2016) similar to loosely defined, mesenchymal stem cells (MSCs) (da Silva Meirelles et al. 2006; Dominici et al. 2006; Pittenger et al. 1999). However,

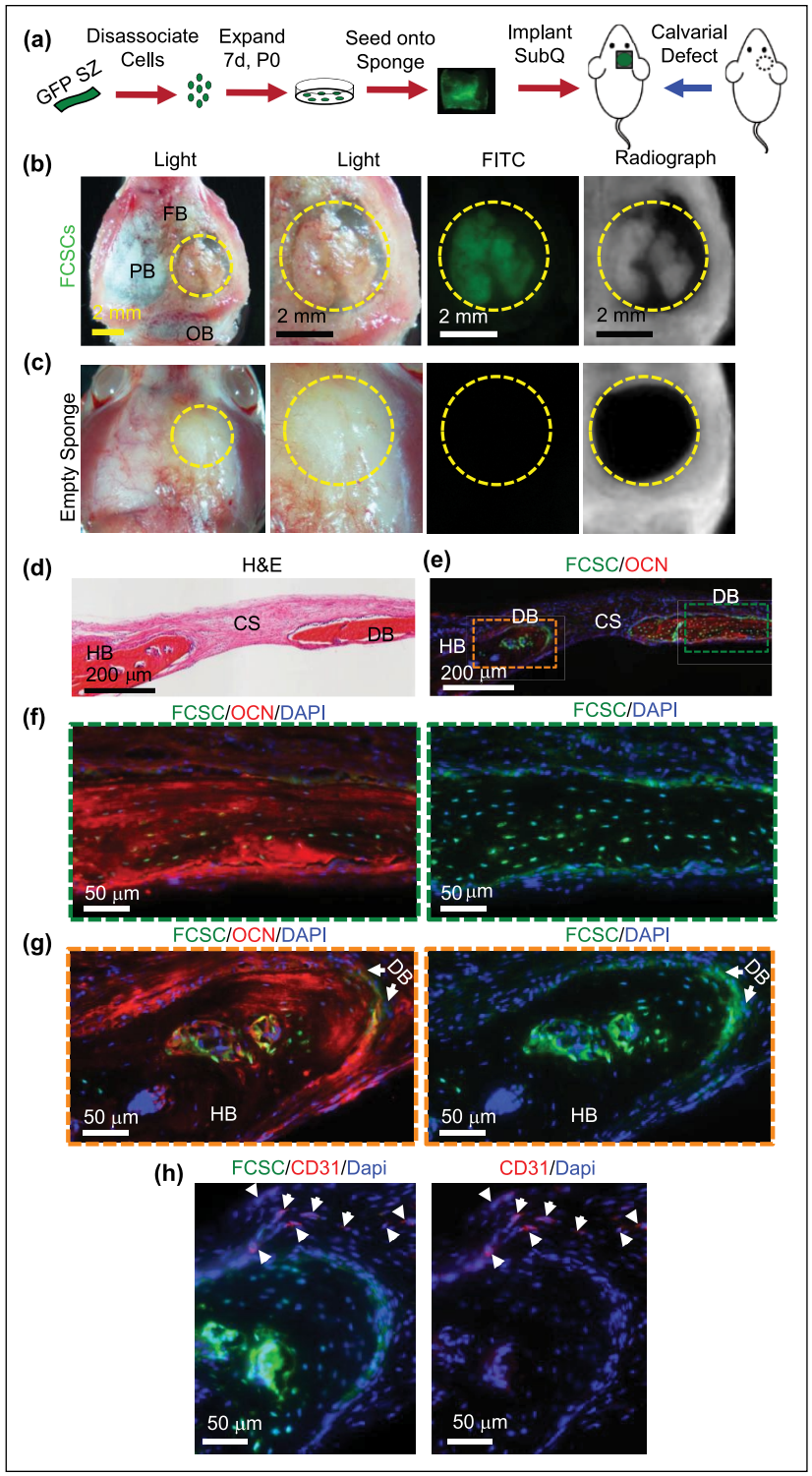

Figure 5. Transplanted GFP$^+$ fibrocartilage stem cells engraft and repair calvarial bone defect. (**a**) Schematic of GFP$^+$ fibrocartilage stem cell (FCSC) transplantation experiment in a mouse calvarial defect model. (**b**) Superior view of nude mouse parietal bone (PB) defect (defect = yellow dashed circle; FB, frontal bone; OB, occipital bone) with transplanted GFP$^+$ FCSCs seeded onto a collagen sponge. FITC microscopy and radiographs demonstrated GFP$^+$ FCSCs and radio-opaque tissue formed within transplants in the calvaria defect. (**c**) Superior view of the nude mouse calvarial bone defect model transplanted with empty sponge negative control. (**d**) Coronal hematoxylin and eosin (H&E) sections of FCSC xenografts (DB, de novo bone; HB, host bone; CS, collagen sponge). (**e–g**) Immunohistochemistry showed donor GFP$^+$ FCSCs engrafted into a host calvarial bone defect and formed de novo bone (GFP$^+$, osteocalcin$^+$). Green = FCSCs; red = osteocalcin; blue = DAPI. (**h**) Immunohistochemistry showed host CD31$^+$ endothelial cells localized at the periphery of newly formed bone. Green = FCSCs; red = CD31.

studies have shown these markers to be exhaustively expressed in MSCs derived from multiple types of connective tissue (da Silva Meirelles et al. 2006), such as skeletal muscle and placenta, which share little functional capacity and dissimilar developmental origin from TMJ-derived FCSCs (Chai et al. 2000). Thus, it is unlikely that classical MSC markers provide any significant specificity or function for FCSCs. Moreover, the existence of a common, ubiquitous MSC is impossible given well-established developmental biology norms (Bianco and Robey 2015; Sacchetti et al. 2016; Robey 2017). To fully understand the regulation of TMJ-derived FCSC function and behavior, it is imperative that we identify specific maker/markers for FCSCs.

Unlike broadly defined MSCs (Pittenger et al. 1999; Dominici et al. 2006), BMSCs are like FCSCs (Embree et al. 2016) given both cell types demonstrate a more rigorous, functional capacity to form heterotopic bone and organize a hematopoietic microenvironment in vivo at a single cell level (Sacchetti et al. 2007; Bianco and Robey 2015; Robey 2017). While sharing this property, it is unlikely that FCSCs are the same cell as BMSCs based on their different developmental origin (Chai et al. 2000; Berendsen and Olsen 2015) and niche (Sacchetti et al. 2007; Embree et al. 2016). In addition, a key functional difference between FCSCs and BMSCs is the spontaneous formation of FCSC-derived cartilage anlagen in our ectopic transplantation model (Embree et al. 2016). Thus, unlike BMSCs, which have to be coerced to form cartilage (Serafini et al. 2014), FCSCs are innately programed to generate cartilage (Embree et al. 2016).

We speculate that the inherent capacity of FCSCs to form cartilage contributed to the delay of angiogenesis in our ectopic xenograft model and to the less robust sprouts in our FIBA experiment. Given proliferating chondroblasts and chondrocytes inhibit angiogenesis through factors such as Chondromodulin-I, Tenomodulin, and Sox-9 (Bi et al. 1999; Shukunami and Hiraki 2007; Hattori et al. 2010), it is plausible that as FCSCs differentiate into chondrocytes, angiogenesis is inhibited and/or delayed. Thus, the secretion of antiangiogenic factors may allow FCSCs to initially form cartilage in our transplantation model. Conversely, terminally differentiated hypertrophic chondrocytes promote angiogenesis through hypoxia-inducible factor 1 (HIF) and VEGF signaling (Carlevaro et al. 2000; Schipani et al. 2009; Sivaraj and Adams 2016). In corroboration of this idea, FCSC-derived cartilage transitioned into vascularized bone-like tissue at 4 wk following transplantation. Moreover, FCSCs cultured at full competency secreted an abundance of VEGF-A, and FCSC-CM induced proliferation of HUVECs.

Finally, we showed that direct FCSC-HUVEC contact enhanced differentiation of FCSCs into osteoblasts, while FCSCs with no HUVEC contact showed no increase in osteogenesis. These data suggest that direct FCSC-HUVEC interaction provides the cues to switch FCSCs' fate from cartilage to bone instead. In support of this idea, we showed that FCSCs transplanted directly into a vascularized bone defect bypassed forming cartilage anlagen and instead engrafted and formed intramembranous bone. Thus, within the vascularized bone niche, FCSCs' access to directly interact with endothelial cells promotes FCSC fate decisions toward bone. Endothelial cell notch activity may mediate FCSC-derived bone formation (Ramasamy et al. 2014). Direct FCSC-HUVEC association also led to an increase in vessel caliber, where FCSCs surrounded lumenized blood vessels. Thus, FCSCs may function to stabilize new blood vessels in FCSC-derived bone (Tattersall et al. 2016). Taken together, we show that the interplay between FCSCs and endothelial cells plays a dynamic and complex role in mediating FCSC-derived bone formation.

Author Contributions

J. Nathan, contributed to design and data acquisition, drafted the manuscript; A. Ruscitto, contributed to design, data acquisition, and analysis, critically revised the manuscript; S. Pylawka, contributed to design, data acquisition, and analysis, critically revised the manuscript; A. Sohraby, contributed to data acquisition and analysis, critically revised the manuscript; C.J. Shawber, contributed to data interpretation, critically revised the manuscript; M.C. Embree, contributed to conception, data acquisition, analysis, and interpretation, drafted and critically revised the manuscript. All authors gave final approval and agree to be accountable for all aspects of the work.

Acknowledgments

This investigation was supported by National Institutes of Health (NIH) grant 5R00DE0220660 (to M.C.E.), Columbia University Provost Faculty Diversity Award (to M.C.E.) and Columbia University College of Dental Medicine. FACS was performed in the CCTI Flow Cytometry Core with the assistance of Dr. Siu-Hong Ho, supported by NIH grants S10RR027050 and S10OD0 20056. Confocal microscopy imaging was performed in the Confocal and Specialized Microscopy Shared Resource of the Herbert Irving Comprehensive Cancer Center at Columbia University, supported by NIH grant P30 CA013696 (National Cancer Institute). The authors declare no potential conflicts of interest with respect to the authorship and/or publication of this article.

References

Aalami OO, Nacamuli RP, Lenton KA, Cowan CM, Fang TD, Fong KD, Shi YY, Song HM, Sahar DE, Longaker MT. 2004. Applications of a mouse model of calvarial healing: differences in regenerative abilities of juveniles and adults. Plast Reconstr Surg. 114(3):713–720.

Berendsen AD, Olsen BR. 2015. Bone development. Bone. 80:14–18.

Bi W, Deng JM, Zhang Z, Behringer RR, de Crombrugghe B. 1999. Sox9 is required for cartilage formation. Nat Genet. 22(1):85–89.

Bi Y, Ehirchiou D, Kilts TM, Inkson CA, Embree MC, Sonoyama W, Li L, Leet AI, Seo BM, Zhang L, et al. 2007. Identification of tendon stem/progenitor cells and the role of the extracellular matrix in their niche. Nat Med. 13(10):1219–1227.

Bianco P, Robey PG. 2015. Skeletal stem cells. Development. 142(6): 1023–1027.

Carlevaro MF, Cermelli S, Cancedda R, Descalzi Cancedda F. 2000. Vascular endothelial growth factor (VEGF) in cartilage neovascularization and chondrocyte differentiation: auto-paracrine role during endochondral bone formation. J Cell Sci. 113(Pt 1):59–69.

Chai Y, Jiang X, Ito Y, Bringas P Jr, Han J, Rowitch DH, Soriano P, McMahon AP, Sucov HM. 2000. Fate of the mammalian cranial neural crest during tooth and mandibular morphogenesis. Development. 127(8):1671–1679.

da Silva Meirelles L, Chagastelles PC, Nardi NB. 2006. Mesenchymal stem cells reside in virtually all post-natal organs and tissues. J Cell Sci. 119(Pt 11):2204–2213.

Descalzi Cancedda F, Melchiori A, Benelli R, Gentili C, Masiello L, Campanile G, Cancedda R, Albini A. 1995. Production of angiogenesis inhibitors and stimulators is modulated by cultured growth plate chondrocytes during in vitro differentiation: dependence on extracellular matrix assembly. Eur J Cell Biol. 66(1):60–68.

Dominici M, Le Blanc K, Mueller I, Slaper-Cortenbach I, Marini F, Krause D, Deans R, Keating A, Prockop D, Horwitz E. 2006. Minimal criteria for defining multipotent mesenchymal stromal cells: the International Society for Cellular Therapy position statement. Cytotherapy. 8(4):315–317.

Duan X, Murata Y, Liu Y, Nicolae C, Olsen BR, Berendsen AD. 2015. Vegfa regulates perichondrial vascularity and osteoblast differentiation in bone development. Development. 142(11):1984–1991.

Embree MC, Chen M, Pylawka S, Kong D, Iwaoka GM, Kalajzic I, Yao H, Shi C, Sun D, Sheu TJ, et al. 2016. Exploiting endogenous fibrocartilage stem cells to regenerate cartilage and repair joint injury. Nat Commun. 7:13073.

Erlebacher A, Filvaroff EH, Gitelman SE, Derynck R. 1995. Toward a molecular understanding of skeletal development. Cell. 80(3):371–378.

Gerber HP, Vu TH, Ryan AM, Kowalski J, Werb Z, Ferrara N. 1999. VEGF couples hypertrophic cartilage remodeling, ossification and angiogenesis during endochondral bone formation. Nat Med. 5(6):623–628.

Hattori T, Muller C, Gebhard S, Bauer E, Pausch F, Schlund B, Bosl MR, Hess A, Surmann-Schmitt C, von der Mark H, et al. 2010. Sox9 is a major negative regulator of cartilage vascularization, bone marrow formation and endochondral ossification. Development. 137(6):901–911.

Kronenberg HM. 2003. Developmental regulation of the growth plate. Nature. 423(6937):332–336.

Lee SH, Che X, Jeong JH, Choi JY, Lee YJ, Lee YH, Bae SC, Lee YM. 2012. Runx2 protein stabilizes hypoxia-inducible factor-1α through competition with von Hippel-Lindau protein (pVHL) and stimulates angiogenesis in growth plate hypertrophic chondrocytes. J Biol Chem. 287(18):14760–14771.

Liang CC, Park AY, Guan JL. 2007. In vitro scratch assay: a convenient and inexpensive method for analysis of cell migration in vitro. Nat Protoc. 2(2):329–333.

Marano JE, Sun D, Zama AM, Young W, Uzumcu M. 2008. Orthotopic transplantation of neonatal GFP rat ovary as experimental model to study ovarian development and toxicology. Reprod Toxicol. 26(3–4):191–196.

Nakatsu MN, Hughes CC. 2008. An optimized three-dimensional in vitro model for the analysis of angiogenesis. Methods Enzymol. 443:65–82.

Pittenger MF, Mackay AM, Beck SC, Jaiswal RK, Douglas R, Mosca JD, Moorman MA, Simonetti DW, Craig S, Marshak DR. 1999. Multilineage potential of adult human mesenchymal stem cells. Science. 284(5411):143–147.

Ramaesh T, Bard JB. 2003. The growth and morphogenesis of the early mouse mandible: a quantitative analysis. J Anat. 203(2):213–222.

Ramasamy SK, Kusumbe AP, Wang L, Adams RH. 2014. Endothelial notch activity promotes angiogenesis and osteogenesis in bone. Nature. 507(7492):376–380.

Robey P. 2017. "Mesenchymal stem cells": fact or fiction, and implications in their therapeutic use. F1000Res. 6:F1000.

Sacchetti B, Funari A, Michienzi S, Di Cesare S, Piersanti S, Saggio I, Tagliafico E, Ferrari S, Robey PG, Riminucci M, et al. 2007. Self-renewing osteoprogenitors in bone marrow sinusoids can organize a hematopoietic microenvironment. Cell. 131(2):324–336.

Sacchetti B, Funari A, Remoli C, Giannicola G, Kogler G, Liedtke S, Cossu G, Serafini M, Sampaolesi M, Tagliafico E, et al. 2016. No identical "mesenchymal stem cells" at different times and sites: human committed progenitors of distinct origin and differentiation potential are incorporated as adventitial cells in microvessels. Stem Cell Reports. 6(6):897–913.

Schenk RK, Wiener J, Spiro D. 1968. Fine structural aspects of vascular invasion of the tibial epiphyseal plate of growing rats. Acta Anat (Basel). 69(1):1–17.

Schipani E, Maes C, Carmeliet G, Semenza GL. 2009. Regulation of osteogenesis-angiogenesis coupling by HIFs and VEGF. J Bone Miner Res. 24(8):1347–1353.

Serafini M, Sacchetti B, Pievani A, Redaelli D, Remoli C, Biondi A, Riminucci M, Bianco P. 2014. Establishment of bone marrow and hematopoietic niches in vivo by reversion of chondrocyte differentiation of human bone marrow stromal cells. Stem Cell Res. 12(3):659–672.

Shibukawa Y, Young B, Wu C, Yamada S, Long F, Pacifici M, Koyama E. 2007. Temporomandibular joint formation and condyle growth require Indian hedgehog signaling. Dev Dyn. 236(2):426–434.

Shukunami C, Hiraki Y. 2007. Chondromodulin-I and tenomodulin: the negative control of angiogenesis in connective tissue. Curr Pharm Des. 13(20):2101–2112.

Sivaraj KK, Adams RH. 2016. Blood vessel formation and function in bone. Development. 143(15):2706–2715.

Tattersall IW, Du J, Cong Z, Cho BS, Klein AM, Dieck CL, Chaudhri RA, Cuervo H, Herts JH, Kitajewski J. 2016. In vitro modeling of endothelial interaction with macrophages and pericytes demonstrates notch signaling function in the vascular microenvironment. Angiogenesis. 19(2):201–215.

Tomo S, Ogita M, Tomo I. 1997. Development of mandibular cartilages in the rat. Anat Rec. 249(2):233–239.

Villars F, Bordenave L, Bareille R, Amedee J. 2000. Effect of human endothelial cells on human bone marrow stromal cell phenotype: role of VEGF? J Cell Biochem. 79(4):672–685.

Vu TH, Shipley JM, Bergers G, Berger JE, Helms JA, Hanahan D, Shapiro SD, Senior RM, Werb Z. 1998. MMP-9/gelatinase B is a key regulator of growth plate angiogenesis and apoptosis of hypertrophic chondrocytes. Cell. 93(3):411–422.

Zelzer E, Mamluk R, Ferrara N, Johnson RS, Schipani E, Olsen BR. 2004. VEGFA is necessary for chondrocyte survival during bone development. Development. 131(9):2161–2171.